3D analysis of the Plasmodium falciparum Maurer's clefts using different electron tomographic approaches.

Marek Cyrklaff, Michael Lanzer, Nicole Kilian, Philipp Henrich

Biotechnology Journal

3D analysis of the Plasmodium falciparum Maurer's clefts using different electron tomographic approaches.

Journal:	*Biotechnology Journal*
Manuscript ID:	biot.200900058.R2
Wiley - Manuscript type:	Technical Report
Date Submitted by the Author:	21-Apr-2009
Complete List of Authors:	Cyrklaff, Marek; University of Heidelberg, Hygiene Institute Lanzer, Michael; Universitätsklinikum Heidelberg, Abteilung Parasitologie Kilian, Nicole; Universitätsklinikum Heidelberg, Abteilung Parasitologie Henrich, Philipp; Universitätsklinikum Heidelberg, Abteilung Parasitologie
Keywords:	Cryo-electron tomography, Maurer's cleft, protein trafficking

Technical Report ((4640 words))

3D analysis of the *Plasmodium falciparum* Maurer's clefts using different electron tomographic approaches.

Philipp Henrich, Nicole Kilian, Michael Lanzer* and Marek Cyrklaff

Hygiene Institut, Abteilung Parasitologie, Universitätsklinikum Heidelberg, Im Neuenheimer Feld 324, 69120 Heidelberg, Germany

*Corresponding author: Michael Lanzer, Abteilung Parasitologie, Universitätsklinikum Heidelberg, Im Neuenheimer Feld 324, 69120 Heidelberg, Germany Phone: ++49 6221 567845; Fax: ++49 6221 564643; E-mail: michael_lanzer@med.uni-heidelberg.de

Keywords: Cryo-electron tomography, Maurer's cleft, protein trafficking

Abbreviations

CEMOVIS – Vitrified sections, Cryo-ET – cryo-electron tomography, MC – Maurer's cleft, PM – Plasma membrane (of erythrocyte), PV – Parasitophorous vacuole, PVM – Parasitophorous vacuole membrane, RBC – red blood cell.

Abstract

The human malaria parasite *Plasmodium falciparum* exports a large number of proteins into its host erythrocyte to install functions necessary for parasite survival. Important structural components of the export machinery are membrane profiles of parasite origin, termed Maurer's clefts. These profiles span much of the distance between the parasite and the host cell periphery and are believed to deliver *P. falciparum*-encoded proteins to the erythrocyte plasma membrane. Although discovered more than a century ago, Maurer's clefts remain a mysterious organelle with little information available regarding their origin, their morphology or their precise role in protein trafficking. Here, we evaluated different techniques to prepare samples for electron tomography, including whole cell cryo-preparations, vitreous sections, freeze-substitution and chemical fixation. Our data show that the different approaches tested all have their merits, revealing different aspects of the complex structure of the Maurer's clefts.

Introduction

Malaria remains a major infectious disease causing over 500 million clinical cases and over one million deaths annually [1]. The high morbidity and mortality of malaria relates to the intra-erythrocytic stages of *P. falciparum* and their ability to sequester in the deep vascular bed of inner organs - resulting in a broad range of pathologies including localized hypoxia, inflammatory reactions and the syndromes associated with maternal and cerebral malaria [2].

By propagating within human erythrocytes, the parasite exploits a unique ecological niche. Human erythrocytes are highly differentiated cells, designed for the key purpose of distributing oxygen within the body. Accordingly, they lack many cellular functions. For example, they are anucleated and transcriptionally- and translationally- inactive; they lack a secretory apparatus; they possess only a limited repertoire of solute and ion transporters and they are readily removed from the circulation when damaged. To survive within such a hostile environment, the parasite has to remodel its adopted host cell by exporting several hundreds proteins into the infected erythrocyte [3]. Some of these proteins alter the biomechanical properties of the host erythrocyte. Other exported proteins create, within the erythrocyte plasma membrane, new permeation pathways for solute uptake and ion regulation [4, 5]. A third group of proteins renders the infected erythrocyte cyto-adhesive or contributes through other means to immune evasion and modulate the severity of the infection [3].

Deleted: sole

To deliver proteins to different destinations within the host erythrocyte, such as the cytoplasm and the plasma membrane, the parasite has to generate a protein export machinery within the host cell – outside the boundaries of its own plasma membrane. A central structural component of this ‘extracellular’ protein export system are Maurer’s clefts [6]. Maurer’s clefts were discovered more than a century ago as stipplings within the cytoplasm of Romanowsky-stained infected erythrocytes [7]. Electron microscopy identified the Maurer’s clefts as stacked unilamellar membrane profiles that appeared electron translucent, and which

were frequently accompanied by vesicle-like structures [8]. Other membrane profiles seen on single ultra-thin sections include whorls, loops and long tubules extending from the parasitophorous vacuolar membrane, which separates the parasite from the cytoplasm of the host cell.

These early micrographs provided only a two-dimensional and thus limited view of the Maurer's clefts, leaving it up to speculation as to whether the different membrane profiles observed in single ultra-thin sections are independent compartments or whether they are connected with each other. Recent studies have attempted to address these issues. Wickert et al. [9] proposed a spatial model of Maurer's clefts on the basis of 3-D reconstructions of consecutive serial sections. According to their model, Maurer's clefts are much more elaborate than is evident from single ultra-thin sections, spanning much of the distance between the parasite and the erythrocyte plasma membrane. Moreover, structures that on single sections appeared separated from each other merged into a continuous membrane network of intertwined tubular and disk-like profiles in the 3D-reconstructions. Electron tomograms confirmed the complex morphology of the Maurer's clefts [10, 11], depicting a single cleft as a flattened, highly buckled sack-like bladder, decorated with nodules and having surface crevices and convoluted edges. Electron-dense tether-like structures seem to connect the Maurer's clefts to the erythrocyte membrane-skeleton [11], consistent with biochemical findings showing that proteins of the Maurer's clefts interact with components of the erythrocyte cytoskeleton [12].

Even though these studies provided novel insights into the fine structure of the Maurer's clefts (reviewed in [13]), a concern remains that these employed exclusively chemical fixation to preserve the specimen. As shown in other systems, chemical fixation can alter the morphology of, or can even destroy, sub-cellular structures [14]. In an effort to overcome these limitations, we have applied four techniques that preserve the sample by rapid freezing

and evaluated the structures by electron tomography. Rapid freezing assures preservation of a sample within milliseconds, and water molecules around and within the sample are immobilized in the original, unordered state, so called vitreous water, without forming crystalline ice [15]. First, we used a whole cells approach, whereby the cells were grown or deposited on EM grids [16,17], plunge frozen and examined at cryo-conditions using an electron microscope. The thinner parts of intact cells could be imaged without necessity of sectioning. Second, we prepared fully hydrated sections, where the material was frozen at high pressure, then sectioned and examined in the EM at cryo-conditions [18]. Third, we generated freeze-substituted sections, where the sample is high-pressure frozen, after which it undergoes a process similar to classical EM preparations including fixation, dehydration, plastic embedding, but under cryo-conditions. The sections were produced at room temperature and examined by EM [19]. Finally we prepared 'Tokuyasu' sections, where chemically fixed material was incubated in high concentrations of sucrose and frozen for sectioning. The sections were then thawed and immunolabelled with specific antibodies coupled to electron dense markers and imaged by EM at room temperature [20]. The Tokuyasu method preserves well the membranes profiles and is particularly suitable for immuno-histological studies. We called the first two approaches a *bona-fide* cryo-EM as these do not involve chemical fixation and also that the samples were in a fully-hydrated vitrified state when examined in the electron microscope at cryo-conditions. The cryo-EM showed novel morphological details of the Maurer's clefts, such as the density in the lumen that is comparable to the exterior, the narrow connections between flat lamellae, as well as that with parasitophorous vacuole, and notably the absence of tethers thought to supposedly interconnect the Maurer's clefts with the plasma membrane of infected cells.

Materials and Methods

The *P. falciparum* strains HB3 and Dd2 were cultured as previously described [21] with some modifications. Briefly, we incubated the parasites in A+ human erythrocytes in Petri dishes of 10 and 25 cm diameter containing HEPES-buffered RPMI medium 10% A+ heat-inactivated human serum and antibiotics. The cultures were incubated in an atmosphere of 3% CO_2, 5% O_2 and 92% N_2, at 37°C and 95% humidity. The cultures were harvested at min of 5% of parasitemia. Preparation for EM: 1. Cryo-electron tomography (Cryo-ET) of perforated, wholly-mounted cells: The parasitized cells (mid trophozoites /schizonts, approx 5% parasitemia) were purified on a magnetic column and perforated using streptolysin O (SLO/Sigma Chemical Co. -St. Louis, MO, USA) (modified after [22], without chemical fixation) to deplete the cytosol. Briefly, we incubated 10^8 cells with 25 units of post-activated SLO for 6 min at RT. Digestion was stopped by putting the sample on ice, and SLO was washed away by 2X centrifuging at 1000g for 2 min and washing with cold PBS, and put in medium for approx. 20 min at RT for cells to recover. 3-4 µl of cell suspension was transferred on holey carbon grid with the fiducial gold markers, the excess of liquid was blotted from the opposite side of the grid and the grids were plunge frozen in liquid ethane at the temperature of -180°C [23]. 2. Cryo-hydrated sections (CEMOVIS): Infected erythrocytes (not permeabilised) were high-pressure frozen using EM PACT2 (Leica Microsystems, Vienna, Austria) at 2000 bars after brief infiltration (2-4 min before freezing) with 20% of 40kD dextran [18]. Thin sections of 80 nm were cut on a Leica microtome at -160°C. 3. Freeze substitution: High pressure freezing – as for CEMOVIS but without dextran. The perfusion of the vitreous samples and slow exchange of bound water with organic solvents (anhydrous acetone) containing 0.1% glutaraldehyde, 0.25% uranyl acetate, and 0.01% osmium tetroxide. Substitution with Lowicryl resins was initiated at -90°C and the

Deleted: The *P. falciparum* strains HB3 and Dd2 were cultured as previously described [21].

temperature was increased by 10°C per hour [19]. Sections of 200 nm were cut at room temperature. 4. Tokuyasu sections: The cells were fixed in 4% formaldehyde, embedded in gelatine, perfused in 2.3 M sucrose and frozen in liquid nitrogen. Frozen blocks were sectioned in a cryo-microtome (Leica EM UC6) at -110°C, thawed on methyl cellulose-sucrose and labelled with STEVOR antibodies followed by 10 nm PA-gold [20].

For EM tomography the samples were examined and tilt series recorded in an FEI Polara electron microscope (Max-Planck-Institute for Biophysics, Frankfurt, Germany), as well as FEI CM300 FEG (Max-Planck-Institute for Biochemistry, Martinsried, Germany), with the acceleration voltage of 300kV. The tomograms were calculated by back-projection of 50-60 images (recorded in the tilt series covering approx ±60°, with 2-3° intervals, and objective lens defocus of 8-14 µm) aligned with fiducial markers (EM processing package [24]). The tomograms for CEMOVIS sections were aligned using cross correlation alignment (ImageJ / plugin: TomoJ) and reconstructed with SIRT (TomoJ). The thickness of Maurer's cleft cisternae was measured between centres of membrane masses in 50 nm intervals along the cisternae. Visualization and surface rendering was done on AMIRA (Visage Imaging GmbH, Berlin).

Deleted:
Deleted: –
Deleted:
Deleted:
Deleted:

Results and Discussion

We first undertook a whole-cell-approach by preparing tomograms of cryo-preserved entire *P. falciparum*-infected erythrocytes. As the electrons transmit through and form an interpretable image only of samples thinner than 0.5-1 µm, it became necessary to partially deplete haemoglobin by perforating the RBC plasma membrane with bacterial toxins. This was achieved with a modified procedure after Jackson et al [22], but without chemically fixing the cells. The resulting tomographic maps of what appeared to be the intact architecture of the infected RBCs covered approx 1-2 cubic microns of cell cytoplasm. Various membrane systems were clearly visible in single sections and in the tomograms. This included the parasite plasma membrane, the parasitophorous vacuolar membrane, the Maurer's clefts and the erythrocyte plasma membrane (Fig. 1A). The knobs (insert in Fig. 1A) appeared as protrusions of the erythrocyte plasma membrane, with a layer of electron dense material underneath. A careful inspection of the tomograms revealed known as well as new features of the Maurer's clefts (Fig. 1B, C and Fig. 2).

Stacks of flat cisternae were observed within the host cell cytoplasm, indicative of Maurer's clefts (Fig. 1B). The lengths of the different cisternae typically varied between 100 and 500 nm and the neighbor lamellae were separated by 30-100 nm of cytoplasm. The lumen of the cisternae was typically 35 nm wide, but could vary between 20 and 200 nm (Fig. 1D). We did not distinguish different classes of Maurer's clefts based on the width of the lamellae. Occasionally some cisternae flattened towards the ends. Apart of the flat lamellae we also observed other membrane morphologies such as whorls that in some tomograms were intermingled with the flat stacks, whereas in some other appeared isolated. Notably, the whorls had a similar distribution of the luminal thickness as the flattened disks (not shown). Moreover, we noted a thickening of the membranes at the main body of the cisternae by

approx. 3 nm, as compared to the ends, due to additional material, possibly of protein origin, attached to the cytoplasmic side of the membrane (Fig. 2A). The cytoplasmic surface of the cisternae had a smooth appearance and the transition between thinner and thicker profiles was smooth, with no detectable abruptions or gaps. Such features were described in classical preparations and referred to as 'electron dense coat' that appears as strongly corrugated material that massively accumulates heavy metal stains [25]. Thick membrane profiles were ubiquitous in the unstained cryo-hydrated preparations that are free of an uncontrolled precipitation of material in random volumes. We regard these densities as a characteristic trait for the Maurer's cleft cisternae. The most typical width of 35 nm was measured predominantly in the regions with thick membrane profiles, which raises the question whether these additional densities endow the characteristic disk shape of the cisternae. We made these measurements on the preparations of whole cells that were perforated before freezing. As this treatment might induce changes in osmolarity [26], which then might affect the volume of cisternae, we made additional measurements on the vitreous sections (CEMOVIS) (along the direction of sectioning), which confirmed the accuracy of the measurements (not shown).

One of the unsolved issues of the Maurer's cleft architecture is whether the cisternae are interconnected with each other, and furthermore, whether they are connected to other membrane compartments of the infected cells [9, 10]. Solving this issue would strongly advance the studies on parasitic protein export [6]. The 3D EM attempts carried out so far on classically prepared samples provided a diverse picture. Wickert et al. [9] described highly interconnected networks of the export machinery, and found connectors to both the parasitophorous vacuole and the plasma membrane of the infected cell. On a contrary, the tomograms of plastic sections showed non-interconnected cisternae, spread in the RBC cytoplasm [11]. The latter study further provided evidence for tethers, potentially proteinaceous connectors between clefts and the plasma membrane of infected RBC.

Our tomograms of cryo-hydrated preparations revealed tubular structures that seemed to interconnect lumina of adjacent cisternae (Fig. 2B). These tubular connectors were shaped like two apposing funnels that merged at the narrowest sites (Fig. 2B). Such interconnections could not be detected between all of the apposing cisternae. The funnel-like connectors were composed of single membranes that lacked the additional protein depositions at the cytoplasmic side, similar to membranous extensions observed at the edges of individual cisternae.

Deleted: 2A

Deleted: 2A

Further, we occasionally observed tubular connections between the Parasitophorous Vacuolar Membrane (PVM) and cisternae (Fig. 2B). The insert in Fig 1A shows a typical distance between the PVM and the plasma membrane of the parasite that is also considered as the minimum distance. Notably, the PVM in cryo-hydrated preparations often appeared at larger distances in respect to the parasite plasma membrane, unlike to that seen in the classical TEM preparations. These differences could be due the osmotic changes [26] after depletion of the excess of hemoglobin for the 'whole cell' preparation. In none of the 16 tomograms examined so far, we could detect membranous connections between the cisternae and the erythrocyte plasma membrane. However, this does not rule out their existence. The cisternae consistently ended well below the inner leaflet of the erythrocyte plasma membrane. Moreover, in one case we detected a seemingly proteinaceous density that was attached at one end to a cisterna, but without connecting it to any other structure (not shown). We often observed proteinaceous material scattered in the cytoplasm between the membrane stacks that typically appeared as diffuse clouds (Fig. 2C) rather than the compact tethers that are frequently seen in the classical EM preparations [11]. The discrepancy between different preparations is likely due to the precipitation of material during fixation and dehydration or the selective accumulations of the stain. Nevertheless, such material observed in cryo-preparation could also be remnants of the extracted cytoplasm after cell perforation.

We next investigated the morphology of the Maurer's clefts using cryo-hydrated CEMOVIS sections [18]. CEMOVIS sections are more challenging to produce and image in the cryo-EM, but notably, they allow thicker parts of the cells to be imaged. The resulting tomographic maps represent a true distribution of densities within the sample, as there is no dilution of the haemoglobin prior to freezing. The tomograms recorded from CEMOVIS sections confirmed the overall architecture of the Maurer's clefts as depicted in cryo-preserved whole cells. Again stacks of flattened cisternae were observed (3A and B). Furthermore, the cisternae also flattened at the ends and the membranes were thicker in the main body of the cisternae than at the ends (Fig. 3C).

On the tomograms of the CEMOVIS sections we measured the electron density of different subcellular compartments and determined that both the lumen of the clefts and the surrounding erythrocyte cytosol exhibited comparable densities (Fig. 3A). Our finding contrasts with previous reports, using classical EM techniques, where the lumen of the cisternae appeared electron lucent [11]. This finding suggests that the Maurer's clefts are filled with more material than previously appreciated. Questions remain concerning the composition of the luminal material, its origin, and the possible role in maintaining the shape of the flattened disks.

The two remaining methods of specimen preservation used in this study involve freezing, but at subsequent steps of the preparation procedures the material is dehydrated and imaged in the EM at room temperature. We next examined the morphology of Maurer's clefts in samples prepared by freeze-substitution. To this end, infected erythrocytes were high pressure frozen, chemically fixed, stained with heavy metal salts and then embedded, at cryo-temperatures, in a plastic material that replaced vitreous water. Although the overall morphology of the Maurer's clefts was preserved in the tomograms of freeze-substituted sections (Fig. 4A and

B), there were clear distinctions when compared with *bona fide* cryo-hydrated preparations. First, the clefts appeared consistently less electron dense than the surrounding erythrocyte cytosol. Second, due to unequal deposition of the stain, the characteristic thinning of membranes towards the ends of cisternae was not distinguished. Third, the cytoplasmic surface of the cisternae had a rough and bumpy texture (Fig. 4C). Occasionally, we observed connections between individual cisternae (Fig. 4C) that resembled tethers seen in classical EM preparations [9, 11]; however, we were unable to discern whether or not the lumina were continuous. The advantage of freeze-substitution is that it offers the possibility of immunolabelling as well as the tomography of serial sections [27] to examine larger volumes of the extended membranous networks of the parasite export system.

Finally we examined specimens prepared by the so-called Tokuyasu technique where chemical fixation is followed by freezing. The tomograms of the sections depicted Maurer's clefts as a complex membrane system (Fig. 5A and B). However, little structural detail could be gleaned from these preparations. The texture of the membranes appeared rough and bumpy and the variations in membrane thickness between ends and middle sections of cisternae was not observed. The lumen of the cisternae appeared electron dense.

As shown in other systems, Tokuyasu sections and freeze-substituted sections are better suited for immuno-EM studies [28]. Using parasites expressing a STEVOR-GFP fusion protein, we were able to localize the protein to the Maurer's clefts in Tokuyasu sections (Fig. 5A and B). However, owing to the size of an antibody and the gold label the resolution is approximately 10-15 nm. Thus, for the Maurer's clefts stacks, it would be difficult to determine whether the antigenic sites are located on the membranes or on connectors between the membranes, without statistical analysis [29]. A co-localization of the detected antigenic

sites with other structural details can only be answered by correlation with the bona-fide cryo-preparations.

Conclusions:

In all preparations the general features of the Maurer's cleft were discernible, and the detailed analysis was remarkably advanced in the three-dimensional maps achieved by electron tomography in the frozen-hydrated EM preparations over that of chemically fixed samples. The membranes of the Maurer's clefts viewed in cryo preparations appeared more continuous than anticipated [9, 11]. This also applied to the connections with the other membranous formations in the infected cell, such as the PVM. The lumen of the lamellae had the same electron density as the surrounding cytoplasm, and the proteineous tethers that supposedly connect the lamellae with the plasma membrane of the infected erythrocyte were not detected. Thus, when exploited in a more systematic manner the methods presented here should be capable of addressing critical questions concerning the mechanisms underpinning the export of adhesive factors to the surface of infected cells. This knowledge may facilitate the development of strategies to inhibit protein export and prevent severe malaria-associated complications, such as cerebral and placental malaria.

Acknowledgements:

We thank Stefan Prior for his excellent assistance in sample preparation, electron microscopy and image processing; we also acknowledge Wolfgang Baumeister and Jürgen Plitzko for using the cryo-electron microscopy facility at the MPI for Biochemistry in Martinsried, Germany; Werner Kuehlbrandt and Derryck Mills for using the cryo-electron microscopy facility at the MPI of Biophysics in Frankfurt. We thank Friedrich Frischknecht and Gareth Griffiths for careful reading the manuscript and useful comments. This work was funded by

the European Commission Network of Excellence "Biology and Pathology of Malaria Parasite (BIOMALPAR)", and the DFG Priority Programme 1399 "Host-Parasite Coevolution".

References:

[1] Snow, RW., Guerra, CA., Noor, AM., Myint, HY., *et al.,* The global distribution of clinical episodes of *Plasmodium falciparum* malaria. *Nature* 2005, *434*, 214–217.

[2] Marti, M., Rug, M., Baum, J., Tilley, L., *et al.,* Signal mediated export of proteins from the malaria parasite to the host erythrocyte. *J. Cell. Biol.* 2005, *171*, 587–592.

[3] Hiller, NL., Bhattacharjee, S., van Ooij, C., Liolios, K., *et al.,* A host-targeting signal in virulence proteins reveals a secretome in malarial infection. *Science* 2004, *306*, 1897-8.

[4] Kirk, K., Membrane transport in the malaria-infected erythrocyte. *Physiol Rev.* 2001, *81*, 495-537.

[5] Ginsburg, H., The permeability properties of the parasite cell membrane. *Novartis Found Symp.* 1999*, 226,* 99-108.

[6] Lanzer, M., Wickert, H., Krohne, G., Vincensini, L., *et al.,* Maurer's clefts: a novel multi-functional organelle in the cytoplasm of *Plasmodium falciparum*-infected erythrocytes. *Int. J. Parasitol.* 2006, *36*, 23-36.

Formatted: German (Germany)

[7] Maurer, G., Die tupfelung der wirtszelle des tetrianaparasiten. *Centralbl. F. Bakt. Abt. I.* 1900, *28*, 114-125.

[8] Aikawa, M., *Plasmodium*: the fine structure of malaria parasites. *Exp. Parasitol.* 1971, *30*, 284-320.

[9] Wickert, H., Göttler, W., Krohne, G., Lanzer, M., Maurer's cleft organization in the cytoplasm of *Plasmodium falciparum*-infected erythrocytes: new insights from three-dimensional reconstruction of serial ultrathin sections. *Eur. J. Cell Biol.* 2004, *83*, 567-82.

[10] Hanssen, E., Sougrat, R., Frankland, S., Deed, S., *et al.,* Electron tomography of the Maurer's cleft organelles of *Plasmodium falciparum*-infected erythrocytes reveals novel structural features. *Mol. Microbiol.* 2008, *67*, 703-18.

[11] Tilley, L., Sougrat, R., Lithgow, T., Hanssen, E., The Twists and Turns of Maurer's Cleft Trafficking in *P. falciparum*-Infected Erythrocytes. *Traffic* 2008, *9*, 187–197.

[12] Blisnick, T., Morales Betoulle, ME., Barale, JC., Uzureau, P., et al., Pfsbp1, a Maurer's cleft Plasmodium falciparum protein, is associated with the erythrocyte skeleton. *Mol. Biochem. Parasitol*. 2000, *111*, 107-121.

[13] Frischknecht, F., Lanzer, M., The *Plasmodium falciparum* Maurer's clefts in 3D. *Mol. Microbiol.* 2008, *67*, 687-691.

[14] Al-Amoudi, A., Dubochet, J., Norlén, L., Nanostructure of the epidermal extracellular

space as observed by cryo-electron microscopy of vitreous sections of human skin. *J. Invest. Dermatol.* 2005, *124*, 764-777.

[15] Dubochet, J., Adrian, M., Chang, JJ., Homo, JC., *et al.,* Cryo-electron microscopy of vitrified specimens. *Q Rev Biophys.* 1988, *21*, 129-228.

[16] Lučić, V., Förster, F., Baumeister, W., Structural studies by electron tomography: from cells to molecules. *Ann. Rev. Biochem.* 2005, *74*, 833-865.

[17] Garvalov, BK., Zuber, B., Bouchet-Marquis, C., Kudryashev, M., *et al*., Luminal particles within cellular microtubules. *J. Cell Biol.* 2006, *174*, 759–765.

[18] Al-Amoudi, A., Norlen, LP., Dubochet, J., Cryo-electron microscopy of vitreous sections of native biological cells and tissues. *J. Struct. Biol.* 2004, *148*, 131-135.

[19] Studer, D., Michel ,M., Muller, M., High pressure freezing comes of age. *Scanning Microsc. Suppl.* 1989, *3*, 253–268.

[20] Griffiths, G., Fine structure immunocytochemistry. Springer Verlag, Heidelberg, Germany, 1993.

[21] Trager, W., Jensen, J.B. Human malaria parasites in continuous culture. *Science* 1976, *193*, 673–675.

[22] Jackson, K.E., Spielmann, T., Hanssen, E., Adisa, *et al.,* Selective permeabilization of

the host cell membrane of *Plasmodium falciparum*-infected red blood cells with streptolysin O and equinatoxin II. *Biochem. J.* 2007, *403*, 167–175.

[23] Cyrklaff, M., Kudryashev, M., Leis, A., Leonard K., *et al.,* Cryoelectron tomography reveals periodic material at the inner side of subpellicular microtubules in apicomplexan parasites. *J. Exp. Med.* 2007, *204*, 1281-1287.

[24] Hegerl, R., The EM Program Package: A Platform for Image Processing in Biological Electron Microscopy *J. Struct. Biol.* 1996, *116*, 30-34.

[25] Atkinson, CT., Aikawa, M., Ultrastructure of malaria-infected erythrocytes. Blood *Cells* 1990, *16*, 351-368.

[26] Lew, VL., Tiffert, T., Ginsburg, H., Excess hemoglobin digestion and the osmotic stability of *Plasmodium falciparum*-infected red blood cells. *Blood* 2003, *101*, 4189-4189.

[27] Höög, JL., Schwartz, C., Noon, AT., O'Toole, ET., *et al.,* Organization of interphase microtubules in fission yeast analyzed by electron tomography. *Dev. Cell* 2007, *12*, 349-361.

[28] Webster, P., Schwarz, H., Griffiths, G., Preparation of cells and tissues for immuno EM. *Methods Cell Biol.* 2008, *88*, 45-58

[29] Vogel, F., Bornhövd, C., Neupert, W., Reichert, A.S., Dynamic subcompartmentalization of the mitochondrial inner membrane. *J. Cell Biol.* 2006, *175*, 237-247.

Figures captions

Fig 1. Cryo-ET of an erythrocyte infected with *Plasmodium* parasite: a whole cell approach. **A**. Low magnification projection image of a cell with plasma membrane perforated before freezing. (Pf – parasite, RBC-PM - erythrocyte plasma membrane, PV - parasitophorous vacuole) Thickness of the cell: RBC cytosol: 300-600 nm, parasite area: >1 µm. Insert-left: zoom-in the other cell where the parasite is located close to the edge of the host erythrocyte, showing different membranes: PVM – parasitophorous vacuole membrane, Pf-PM – parasite plasma membrane. Insert-right: Knobs on the erythrocyte plasma membrane – section through a tomogram. **B.** Slice through a tomogram of another cell showing lamellae of a Maurer's cleft. Thickness of reconstruction: ~400 nm. **C**. Surface rendered volume (light blue) of the same area as in B. **D.** Histogram showing distribution of thickness of the Maurer's cleft lamellae (Scale bars A: 1 µm; A-inserts and B: 100 nm).

Fig 2. Details of Maurer's cleft morphology: a whole cell cryo-EM approach as in Fig 1. **A.** Section through a reconstruction and surface rendered view showing the continuity between thicker (black arrowheads) and thinner (white arrowheads) membranes of the Maurer's cleft. **B.** Tubular connections between parasitophorous vacuole membrane PVM and Maurer's cleft (black arrowhead), and between cisternae of the Maurer's cleft (white arrowhead). Pf – parasite. The inserts below views the same volume at different angle, and a surface rendered view. **C**. Diffused material (presumably protein) filling gaps between the stacks of Maurer's clefts (indicated with arrows). Thickness of cell in A-C: 300-450 nm (Scale bars: 100 nm).

Fig 3. Tomogram of a cryo-hydrated section through the Maurer's cleft. **A.** Section through the tomogram. The lumen of MC (white asterix) has similar density as cytoplasm of RBC

(black asterix). Circle: area shown in C. **B.** Surface rendered lamellae of Maurer's cleft (light blue). **C.** Thick and thin membrane of the Maurer's cleft, area encircled in A (as in Fig. 2A). Thickness of the section: 120 nm. (Scale bar for A,B: 200 nm).

Fig 4. High pressure frozen – freeze substituted cells. **A**. Slice through a tomogram showing lamellae of Maurer's cleft **B.** Surface rendered view of the structures in A. (light blue – Maurer's cleft lamellae, dark blue – erythrocyte plasma membrane, green - parasite). **C.** Connectors (violet) between lamellae (light blue). Thickness of the section: 200 nm. (Scale bars: 200 nm).

Fig 5. 'Tokuyasu' section of infected erythrocyte, immunolabelled against STEVOR. **A.** Section through a tomogram showing morphology of MC and STEVOR labelling. **B.** surface rendered view of the area in A. (blue – Maurer's cleft, dark blue – outline of erythrocyte plasma membrane, green – outline of parasitophorous vacuole, red – positions of gold markers). Thickness of the section: 200 nm. (Scale bar: 200 nm).

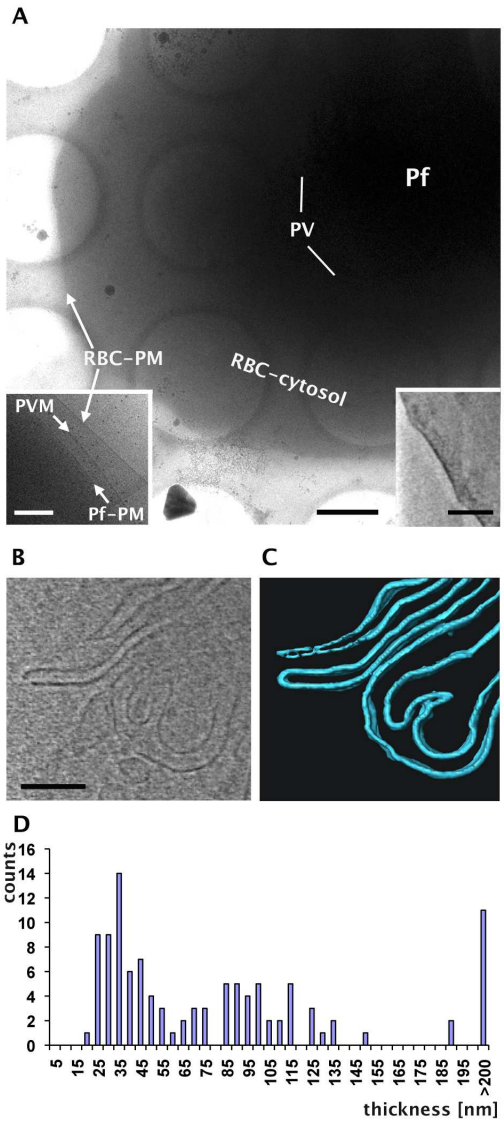

Fig. 1 **Henrich etal 09**

80x189mm (300 x 300 DPI)

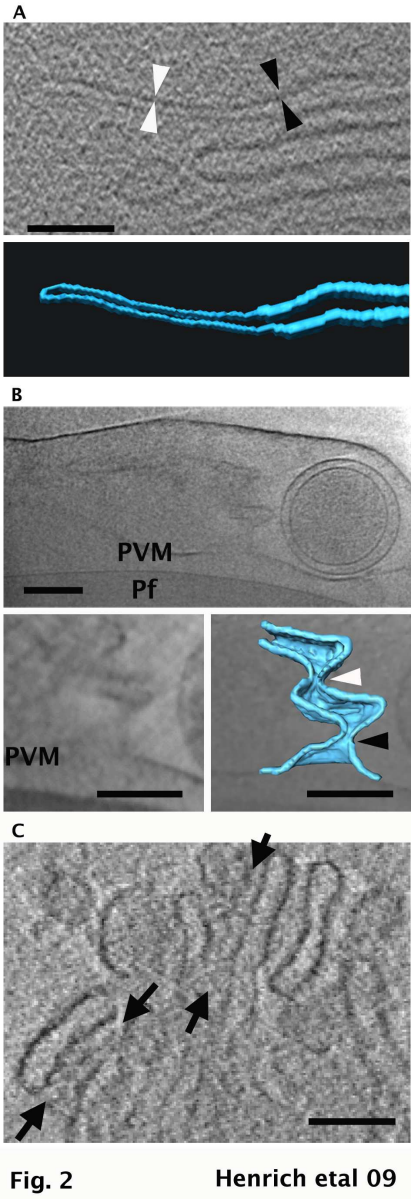

Fig. 2 Henrich etal 09

80x233mm (300 x 300 DPI)

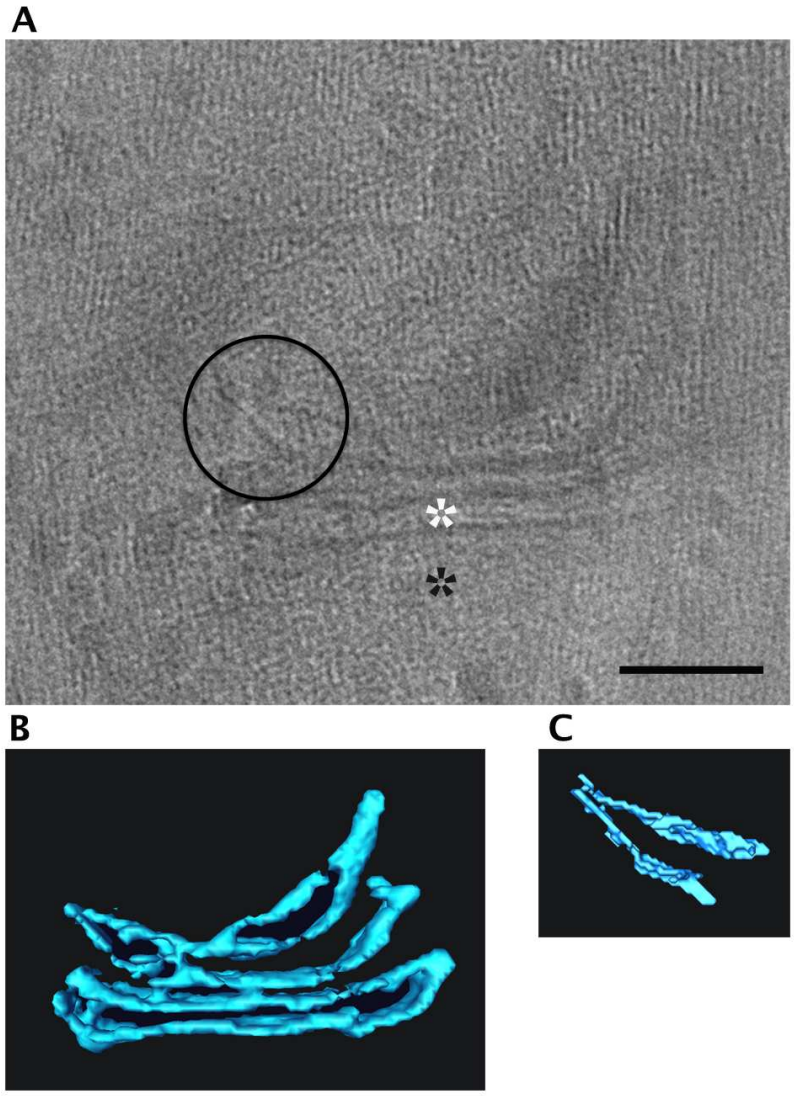

Fig. 3 Henrich etal 09

80x120mm (300 x 300 DPI)

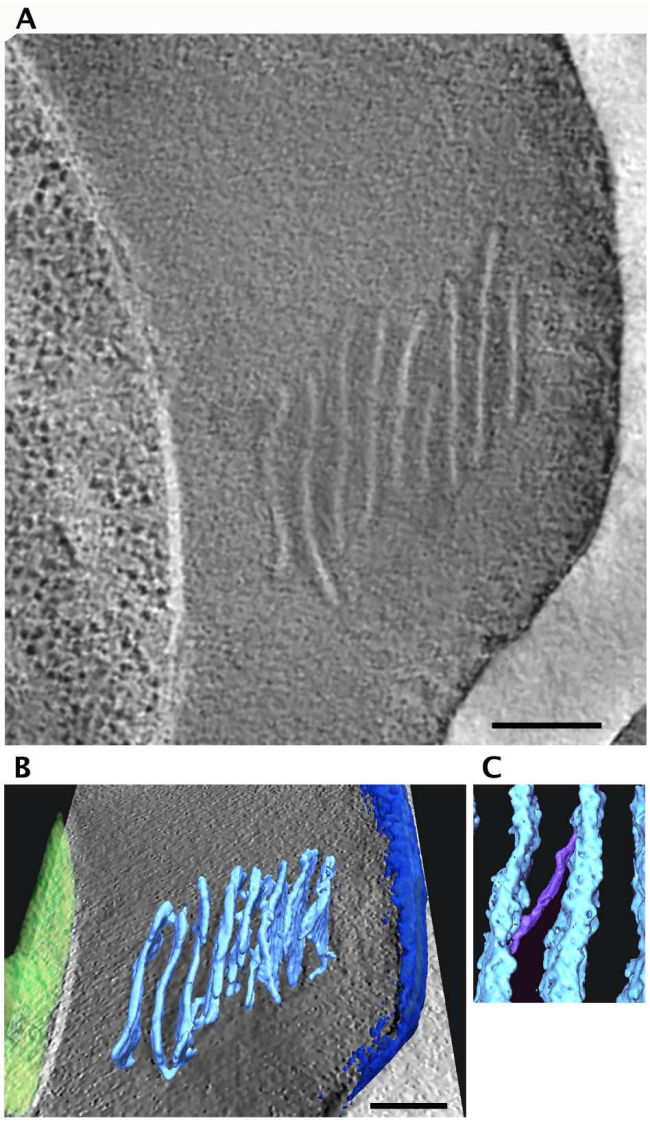

Fig. 4 Henrich etal 09

80x148mm (300 x 300 DPI)

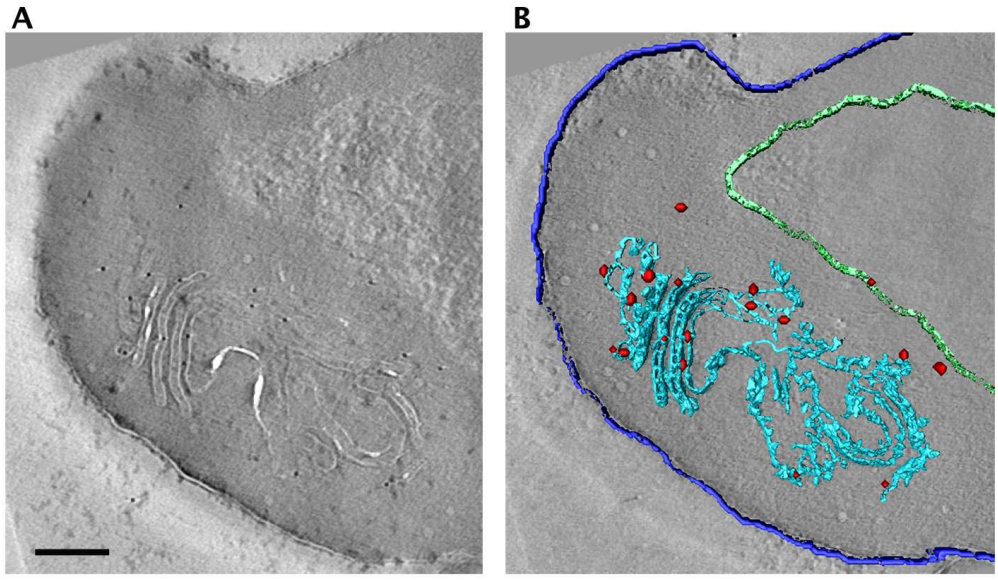

Fig. 5

Henrich etal 09

119x78mm (300 x 300 DPI)